Supplementary material to "Comparison of two Oxidation flow reactors for measuring aged aerosol from passenger car exhaust"

S1 OFR data processing

Residence time distributions are defined as linear combinations of Taylor distributions

$$E(t) = \sum_i \frac{f_i}{2} \exp\left(-\frac{Pe_i(\tau_i - t)^2}{4\tau_i t}\right)\sqrt{\frac{Pe_i}{\pi\tau_i t}}, \quad (S1)$$

where t is time, $\sum_i f_i = 1$ and i goes from 1 to 3 for PAM-OFR and from 1 to 2 for DOFR (Simonen et al., 2024). The parameters are presented in Table S1 and the distributions in Figure S1.

Table S1. Residence time distribution parameters (Simonen et al., 2024)

	PAM-OFR	DOFR
f_1	0.1357	0.5438
f_2	0.3098	0.4562
f_3	0.5545	-
Pe_1	31.8016	59.9304
Pe_2	9.8594	13.9073
Pe_3	6.5239	-
$\tau_1(s)$	33.7762	27.1867
$\tau_2(s)$	59.6120	49.9008
$\tau_3(s)$	159.0658	-

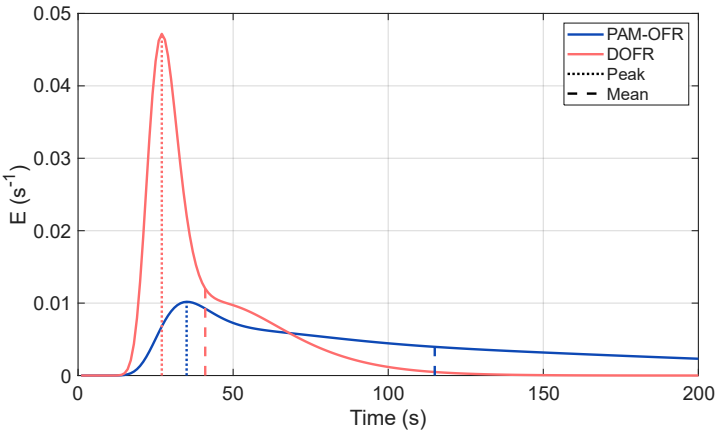

Figure S1. Residence time distributions

In the LVOC fate model (Palm et al., 2016), LVOC molecules are assumed to 1) condense on aerosol particles, 2) fragment after five reactions with OH, 3) stick to OFR walls or 4) exit the OFR in the gas phase. Equilibration time between gas and particle phases comes from

$$\tau_{cond} = \frac{1}{4\pi\, CS\, D}, \quad (S2)$$

where CS is condensation sink and $D = 7 \cdot 10^{-6}\ m^2\ s^{-1}$ is gas diffusion coefficient. CS was estimated from an average PN distribution before and after the OFR. Sticking coefficient of 1 was used in CS calculation. The OH exposure from the PAM Chem model was used in step 2 to estimate OH concentration, and surface area to volume

ratio (25 for the PAM-OFR and 46 for the DOFR) in step 3. For more information, see Palm et al. (2016) and references therein.

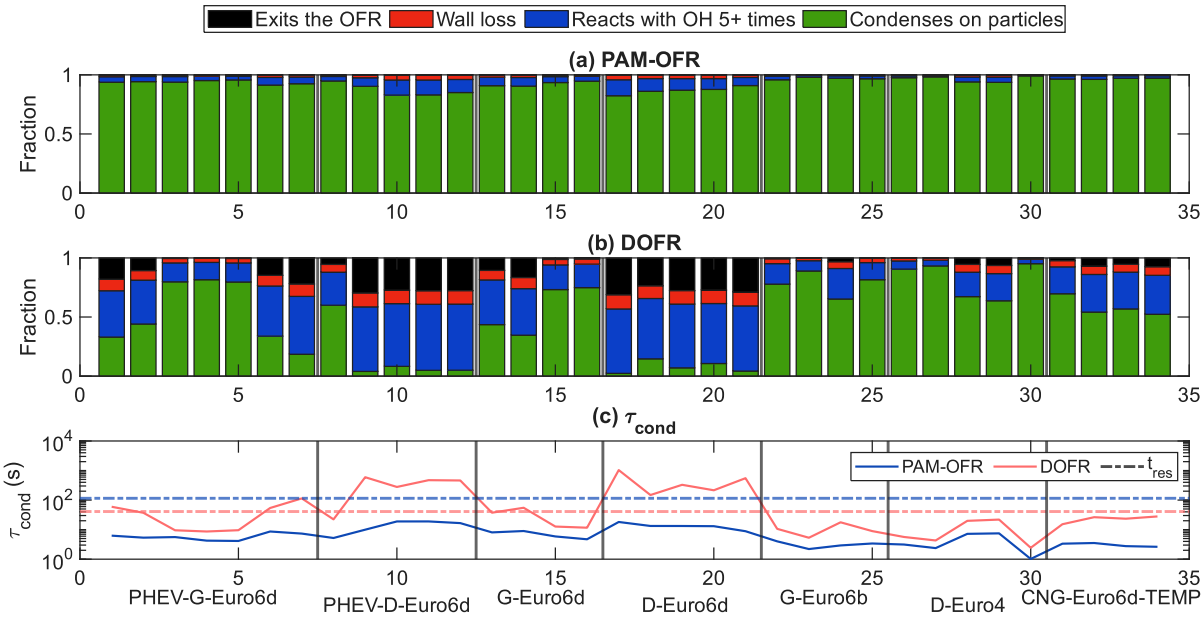

Figure S2. LVOC fate modeled with Palm et. al (2016) algorithm for PAM-OFR (a) and (b) DOFR (b) using the modeled photochemical age for each cycle. Equilibration time for condensation τ_{cond} compared with the residence time (t_{res}) for both OFRs in (c).

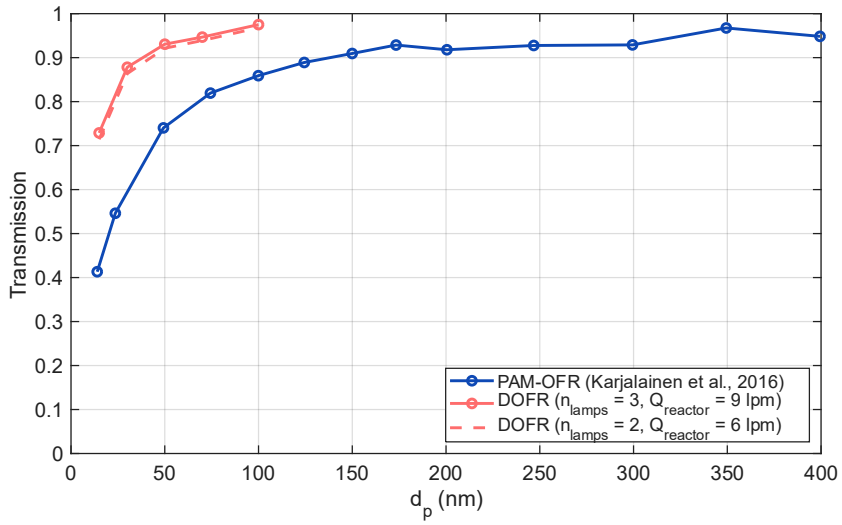

Figure S3. Transmission curves of particles in the OFRs. Transmission measurements were done by Karjalainen et al. (2016) for the PAM-OFR and by Dekati for the DOFR. As with the DOFR the amount of UV lamps and reactor flow were changed during the campaign, both transmission curves are presented here. DOFR transmission curves include losses in the sample conditioning and reactor unit.

S2 ELPI+ results and data processing

Table S2. OH exposures, photochemical ages and secondary particle mass emission factors for all cycles.

		OH exposure (molec. cm^{-3} s^{-1})		Photochemical age (d)		EF (mg km^{-1})	
Cycle index	Temp (°C)	PAM-OFR	DOFR	PAM-OFR	DOFR	PAM-OFR	DOFR
PHEV-G- Euro 6d							
1	35	4.54E+11	4.10E+11	3.50	3.16	10.86	1.62
2	35	4.95E+11	4.64E+11	3.82	3.58	18.22	5.95
3	-9	5.15E+11	4.32E+11	3.97	3.34	18.50	22.51
4	-9	5.28E+11	4.26E+11	4.07	3.28	28.07	24.87
5	-9	4.68E+11	4.35E+11	3.61	3.35	26.14	44.73
6	23	4.73E+11	4.76E+11	3.65	3.68	8.91	7.01
7	23	4.78E+11	4.74E+11	3.69	3.66	6.77	3.83
PHEV-D- Euro 6d							
8[a]	35	4.46E+11	4.29E+11	3.44	3.31	29.19	11.87
9	-9	4.63E+11	4.72E+11	3.57	3.64	8.05	0.77
10	-9	4.68E+11	4.74E+11	3.61	3.66	22.50	6.57
11	23	4.59E+11	4.95E+11	3.54	3.82	3.43	1.70
12	23	4.49E+11	4.97E+11	3.47	3.83	10.09	5.39
G- Euro 6d							
13	35	5.62E+11	4.75E+11	4.34	3.67	6.85	12.78
14	35	5.17E+11	4.24E+11	3.99	3.27	8.62	12.06
15	-9	5.23E+11	4.60E+11	4.03	3.55	13.63	15.53
16	-9	5.31E+11	4.68E+11	4.09	3.61	19.61	17.78
D- Euro 6d							
17	35	5.20E+11	4.61E+11	4.01	3.56	3.76	0.00 [b]
18[a]	35	5.40E+11	4.82E+11	4.17	3.72	4.52	2.59
19	-9	4.87E+11	4.79E+11	3.76	3.70	4.48	3.93
20	-9	4.59E+11	4.54E+11	3.54	3.50	5.83	3.22
21	23	4.90E+11	4.81E+11	3.78	3.71	18.32	0.83
G- Euro 6b							
22	35	4.63E+11	4.30E+11	3.57	3.31	45.23	50.22
23	35	4.08E+11	3.78E+11	3.15	2.91	71.64	56.89
24	-9	4.23E+11	4.58E+11	3.26	3.54	71.00	25.06
25	-9	4.20E+11	4.08E+11	3.24	3.15	48.47	50.44
D- Euro 4							
26	35	3.00E+11	2.77E+11	2.32	2.14	29.74	40.81
27	35	2.70E+11	2.45E+11	2.08	1.89	9.47	8.43
28	-9	3.47E+11	3.17E+11	2.68	2.45	11.34	7.69
29	-9	3.63E+11	3.38E+11	2.80	2.61	24.59	11.09
30	23	3.37E+11	3.31E+11	2.60	2.55	58.85	23.97
CNG-Euro 6d-TEMP							
31	-9	4.72E+11	4.40E+11	3.64	3.39	32.91	17.02
32	-9	4.91E+11	4.57E+11	3.79	3.53	27.63	13.13
33	23	4.61E+11	4.79E+11	3.56	3.69	34.37	12.47
34	23	4.60E+11	4.62E+11	3.55	3.56	37.04	13.51

[a] DPF regeneration during cycle, [b] EF for PM_{fresh} was equal to EF for PM_{aged} within error limits

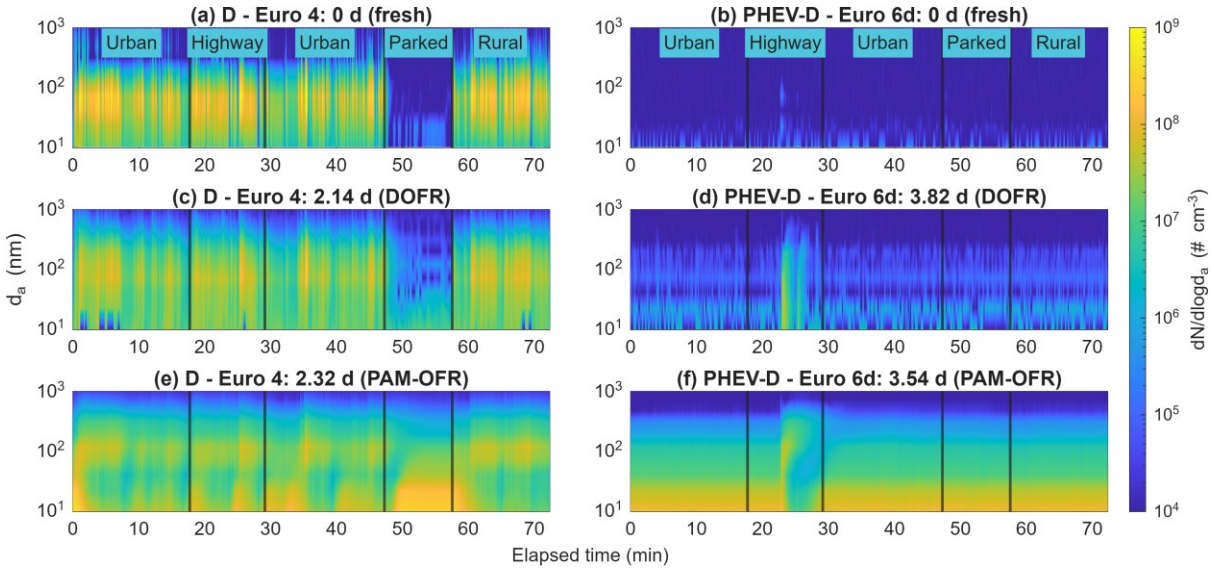

Figure S4. Particle number size distributions as a function of time for the Euro 4 and PHEV Euro 6d diesel cars measured in fresh exhaust (a, b), aged in the DOFR (c, d) and in the PAM-OFR (e, f). The data was corrected for DR and standard temperature, and the cycle indexes are 26 for Euro 4 diesel and 11 for PHEV diesel in Fig. 5 and Table S2. Ages correspond to OH exposures of $2.77 \cdot 10^{11}$ (c), $3.00 \cdot 10^{11}$ (e), $4.95 \cdot 10^{11}$ (d) and $4.59 \cdot 10^{11}$ (f) molec. cm^{-3} s^{-1}.

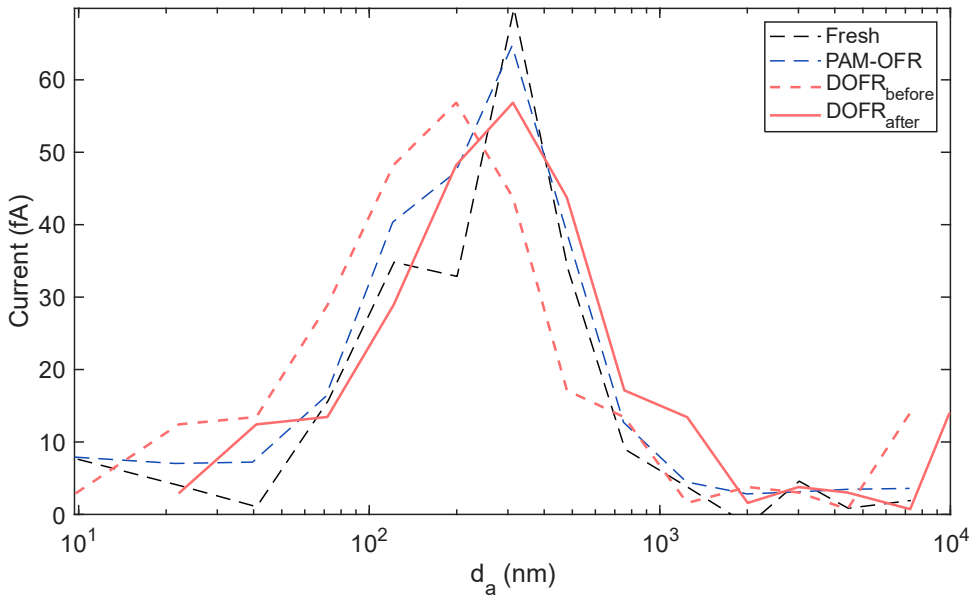

Figure S5. Averaged current distributions from the ELPI+ comparison measurement with room air. DOFR cut-off sizes were changed based on this measurement.

References

Palm, B. B., Campuzano-Jost, P., Ortega, A. M., Day, D. A., Kaser, L., Jud, W., Karl, T., Hansel, A., Hunter, J. F., Cross, E. S., Kroll, J. H., Peng, Z., Brune, W. H., and Jimenez, J. L.: In situ secondary organic aerosol formation from ambient pine forest air using an oxidation flow reactor, Atmos. Chem. Phys., 16, 2943–2970, https://doi.org/10.5194/acp-16-2943-2016, 2016.

Simonen, P., Dal Maso, M., Prauda, P., Hoilijoki, A., Karppinen, A., Matilainen, P., Karjalainen, P., and Keskinen, J.: Estimating errors in vehicle secondary aerosol production factors due to oxidation flow reactor response time. Atmos. Meas. Tech., 17, 3219–3236, https://doi.org/10.5194/amt-17-3219-2024, 2024.